Reversible integration of microfluidic devices with microelectrode arrays for neurobiological applications

Konstantin Grygoryev [a], Grégoire Herzog [b], Nathan Jackson[a], Jörg Strutwolf[e], Damien W.M. Arrigan [c], Kieran McDermott [d], Paul Galvin [a]

a) Tyndall National Institute, Lee Maltings, Prospect Row, Cork, Ireland
Email: konstantin.grygoryev@tyndall.ie; Telephone: +353214906884

b) Lorraine University, LCPME: Laboratory of Physical Chemistry and Microbiology for the Environment, 405, Rue de Vandoeuvre, 54601 Villers-lès-Nancy, France

c) Nanochemistry Research Institute, Department of Chemistry, Curtin University, GPO Box U1987, Perth, WA 6845, Australia

d) University College Cork, Department of Anatomy, Western Gateway Building, Western Road, Cork, Ireland

e) Institute of Organic Chemistry, University of Tübingen, Auf der Morgenstelle 18, 72076 Tübingen, Germany

1 Abstract

The majority of current state of the art microfluidic devices are fabricated via replica molding of the fluidic channels into PDMS elastomer and then permanently bonding it to Pyrex surface using plasma oxidation. This method presents a number of problems associated with the bond strengths, versatility, applicability to alternative substrates and practicality. Thus, the aim of this study was to investigate a more practical method of integrating microfluidics which is superior in terms of bond strengths, reversible and applicable to a larger variety of substrates, including microfabricated devices.

To achieve the above aims, a modular microfluidic system, capable of reversible microfluidic device integration, simultaneous surface patterning and multichannel fluidic perfusion, was built.

To demonstrate the system's potential, the ability to control the distribution of A549 cells inside a microfluidic channel was tested. Then, the system was integrated with a chemically patterned microelectrode array, and used it to culture primary, rat embryo spinal cord neurons in a dynamic fluidic environment.

The results of this study showed that this system has the potential to be a cost effective and importantly, a practical means of integrating microfluidics. The system's robustness and the ability to withstand extensive manual handling has the additional benefit of reducing the workload. It also has the potential to be easily integrated with alternative substrates such as stainless steel or gold without extensive chemical modifications. The results of this study are of significant relevance to research involving neurobiological applications, where primary cell cultures on microelectrode arrays require this type of flexible integrated solution.

1 Introduction

Microelectromechanical systems (MEMS) are small devices aimed towards miniaturization of experiments and methods of collecting data. The current state of the art MEMS devices can be very complex, highly engineered and often integrate surface chemistry modifications and microfluidics with other micro-fabricated components [e.g. 1, 2, 3].

Microfluidics is a technology and field of research where relatively small volumes of fluids are pumped through channels of micrometer scale [4]. Flow of fluids of such low volumes is dominated by surface tension, viscosity, surface area to volume ratio and diffusion.

The combination of these factors results in laminar flow, where separate streams of fluid can flow side by side with out turbulent mixing [5].

The interest in microfluidics stemmed from the demand for miniature devices, capable of performing chemical analysis. Even though systems such as gas chromatography (GC) and high pressure liquid chromatography (HPLC) provided high sensitivity and resolution of chemical composition, these systems were limited for laboratory use only. Hence, in the attempt to perform similar analysis on a micro-scale, outside of the laboratory, the research and development of microfluidic technology begun [6].

Microfluidic (μF) devices are essentially microscopic networks of fluidic channels. These channels can be etched into glass [7], silicon [8] moulded into a block of structural polymer such as cyclic-olefin copolymer (Zeonor) [9], poly-methyl methacrylate (PMMA) [10] or photo curable perfluoropolyether (PFPE) [11, 12]. Additional materials suitable for fabrication of μF devices are described in the review article by Nge et, al. [13]. The design and dimensions of these devices as well as choice of base material is governed by the experimental requirements and cost. For example, experiments involving biological cell cultures require that the μF device and the substrate are optically transparent and compatible with light and fluorescent microscopy. Materials such as polydimethyl(siloxane) (PDMS) and Pyrex fit these criteria. PDMS is by far the most common material used for fabrication of μF devices. The common listed attributes of PDMS are its low cost, high transparency, good surface conformity, gas permeability, solvent resistance and bio-compatibility [14, 15]. Using PDMS, a new μF device can be made within 90 minutes, provided that the masters are available.

In order for the μF device to function as intended, the micro-channel network must be sealed by bonding it to another surface. For example, 3D devices can be made by aligning and bonding one μF device to a second device with a complementary network [16, 17]. The most common approach however, is to permanently bond the μF device to a Pyrex slide or coverslip. This bond is achieved by plasma oxidation of both surfaces followed by alignment and conformal contact [18]. The permanency of the bond between the PDMS μF device and its substrate is generally desired, seemingly providing a watertight seal; however, it becomes a limiting factor when used with expensive, complex substrates such as microelectrode arrays (MEAs) [19]. MEAs are micro-fabricated devices used for collecting electrophysiological data from neurons or cardiomyocytes [20]. Due to their sensitivity to changes in surface chemistry (apart from the standard coating with cytophilic compounds e.g. PLL or fibronectin) the scope of application is narrow. Permanent modification of these devices further decreases applicability, resulting in a costly device with

single, specific application. The limitation of the permanent bond becomes more apparent if the μF fails and detaches from the surface. This leaves the MEA permanently contaminated with portions of PDMS. The contaminating PDMS can be dissolved using, for example, a solution of tetra butyl ammonium fluoride (TBAF-75% wt. in water) [21]. However, this can result in coating the entire MEA with PDMS as it re-adsorbs to the surface from the TBAF solution [22-24]. Since PDMS is also an electrical insulator, the adsorption of PDMS can increase the microelectrode impedance, making them insensitive to cellular electrical [24, 25].

The second limitation of permanent μF integration is related to *patterned* surface chemistry modifications and cell culture [26, 27]. In addition to chemical bonding, plasma treatment is primarily used to remove organic surface contaminants; hence, patterning of cell adhesion proteins (e.g. laminin, fibronectin or streptavidin) prior to plasma treatment, will be ineffective as the protein will be etched from the surface [28]. Additionally, the plasma treated surfaces, such as polystyrene or silicon nitride passivation, become cytophilic, preventing the biological cells from distinguishing between the protein pattern and the non-patterned, "background" surface [29].

Lastly, to date there has been a large number of devices built through integration of MEA with either microfluidics or patterned surface chemistry [30-32]. However, there are limited numbers of studies attempting to integrate all three components into a single device [33].

Hence, the aim of this study was to design and build a modular system which allows simultaneous, integration of microfluidic devices with chemically patterned MEAs and neuronal cell culture. To achieve this level of integration, the μF devices were attached in reversible manner, relying on mechanical force, rather than chemical bonds to create a functional fluidic network. Substituting the PDMS bonding method allowed the patterning of the MEA surface chemistry. Furthermore, the reversible nature of the μF device integration makes it easy to add or remove the microfluidic element at the desired stage of an experiment.

Such a system has the potential to expand the scope of MEA application, making these devices suitable for simultaneous experiments with surface chemistry, microfluidics, tissue culture and electrophysiology. In addition, our goal was to ensure that this system was practical in terms of its size and complexity, and that it could withstand regular use and manual handling.

To demonstrate the feasibility of our strategy, we used this system for the culture of A549 cells in a differential microfluidic environment and for the multichannel perfusion of a patterned, primary neuronal culture on the surface of an MEA.

2 Materials & Methods

2.1 Materials

Fibronectin, poly-D-lysine (PDL), fluorescein isothiocyanate tagged poly-L-lysine and Terg-a-zyme were purchased from Sigma-Aldrich, U.K. B-27 supplement, Dulbecco's Modified Eagles Media (DMEM), GlutaMAX, Hank's balanced salt solution foetal Bovine Serum (FBS) and Neurobasal media were all

purchased from Invitrogen, USA via Bio-Sciences, Ireland. Single sided adhesive, polymerase chain reaction film, AB 0558 was purchased from Thermo Scientific, Germany. PDMS (Sylguard 184) was purchased from Dow Corning, UK. Biocompatible double-sided pressure sensitive adhesive tape, Orabond 1397PP was purchased from Orafol, Germany. Halogenated ether (Isoflow) used for rodent anesthesia was supplied by Dept. of Anatomy.De-ionised (DI) water was purified using an Elga Purelab Ultra (Ultra Genetic) water purification system (Veolia Water Systems, Ireland). The de-ionised water used throughout had resistivity of 18.2 MΩ·cm. The MEAs, the alignment set-up, poly(methyl methacrylate) and Nylon culture rings were all fabricated in house at Tyndall National Institute. The cell culture and the µF device perfusion was performed using a KD Scientific 410-CE syringe pump. The imaging was performed using inverted microscopes Olympus IX70 or Olympus IX50. Both microscopes were equipped with DP70 and DP12 digital cameras respectively. Eppendorf 5810 centrifuge was used to separate the cell suspension.

2.2 The basic steps of µF system integration

1) MEA fabrication
2) Fabrication of the culture chamber, the µF device module and the reservoir module
3) MEA integration with the culture chamber
4) MEA Surface chemistry modification (coating or patterning)
5) Cell culture
6) Attachment of the µF device to the MEA
7) Perfuse the culture for a predetermined amount of time.

2.3 The design process

Our aim was to use the MEA as the foundation to build a system which would simultaneously allow the culturing of primary neurons, study the effects of surface chemistry patterning (patterned cell adhesion)and microfluidic perfusion, and record electrophysiological activity of the cultured cells.

The MEA is simply an interface between the electrically active neuronal cells and a set of amplifiers; hence, it was paramount that the integration of the microfluidics did not interfere with data collection or the associated hardware (hot-plate, amplifiers and the PC). The key consideration was the outer diameter of the cell culture ring as it has to fit through the designated opening of the amplifier (r=1.5 cm). Hence, it was insured that the dimensions of the set-up were kept with-in this limit.

Initially, a number of methods of coupling the µF devices to the MEAs were investigated These tests included the conventional plasma bonding (32 W, 900mTorr for 1 min) and bonding using two bio-compatible, UV-cure cyanoacrylates (Dymax 1-20791 and Norland NOA 68 cured for 20 min using the BioForce UV cleaner). However, these methods were insufficient for long-term use. The plasma bonded devices were very prone to leaks, while the cyanoacrylates, although initially showing a relatively strong bond, failed after two or three days when perfused with cell culture media. More importantly, all of the above methods left the substrates permanently altered with chemically bound PDMS or acrylic adhesive.

153 However, even if permanent bonding was a reliable method, it would have made it difficult to chemically
154 pattern the surface either prior or after the µF integration. Hence, our solution was to devise a method of
155 reversibly coupling the µF device to the MEA (see sections: 2.4.3, 2.4.4 and 2.4.5).
156 The patterning of the MEA for the purposes of clustering cell adhesion on and around the microelectrodes
157 presented different constraints. As the MEA is an electrical interface, the quality of the signal delivered to
158 the amplifier is greatly influenced by the electrode surface chemistry. Permanent modifications, such as
159 accidental PDMS adsorption which occurs during a process of micro-contact printing (µCP) for example,
160 increases the electrode impedance and noise (see supplementary section S.5). Hence, to limit the exposure
161 of the electrodes to the PDMS, the surface patterning was performed using the specifically designed, µF
162 device. The fluidic channel network of this device corresponded to the layout of the microelectrodes on the
163 MEA. This method ensured that the microelectrodes did not come into direct contact with PDMS during
164 PDL-fibronectin perfusion.

165 ## 2.4 Fabrication steps

166 ### 2.4.1 Silicon masters

167 The µF devices used for this study were fabricated by replica molding of PDMS against a silicon master.
168 Two sets of etched silicon masters were fabricated in-house using the Bosch process [34]. The detailed
169 fabrication protocol is outlined in the supplementary section S.1.
170 One set of masters was intended for surface patterning (**Fig. 1**(a)), the second set was used to fabricate the
171 µF devices for cell culture perfusion (**Fig. 1**(b)). Initially, the surface patterning was intended to be carried
172 out via micro-contact printing (µCP) rather than µF patterning. However, after a comparison between the
173 two methods, µF patterning proved to be more consistent producing uniform pattern features; hence, it was
174 chosen as the preferred method (see supplementary section S.4)
175 The dimensions of the masters were as follows: the master for patterning was 4.8 mm in diameter and
176 featured a grid of circular chambers (r=30 µm, h=15 µm, 200 µm apart) interconnected with short channels
177 (w=20 µm, h=15 µm). This layout directly corresponded to the microelectrodes on the MEA. The master
178 for perfusion µF had a diameter of 1.7 cm, with a 2000 (W) x 5000(L) x 100 (H) µm central channel and
179 two perpendicular 600 µm wide inlets. To ensure that the described design was suitable for generating
180 laminar flow and microfluidic gradients, a COMSOL computational fluid dynamics (CFD) simulation was
181 performed.
182 Following the CFD simulation, the masters were fabricated and prepared for PDMS replica molding. The
183 masters were silanized with Tridecafluoro-1,1,2,2-tetrahydrooctyl-1-trichlorosilane (TFOCS) as previously
184 described [35-37]. This layer served as an effective release agent for PDMS. Briefly, the silanization with
185 TFOCS was performed inside a desiccator at RT. First, lint-free tissue was placed inside the desiccator and
186 soaked with 2-3 drops of TFOCS. Then, the silicon masters were then placed in the desiccator and air was
187 evacuated for 1 min. The reduced pressure induced the evaporation of TFOCS. The vacuum was then
188 turned off and the masters were left in the sealed desiccator for 30 min. The TFOCS formed a monolayer
189 on the master surface via siloxane bonding, resulting in increased surface hydrophobicity.

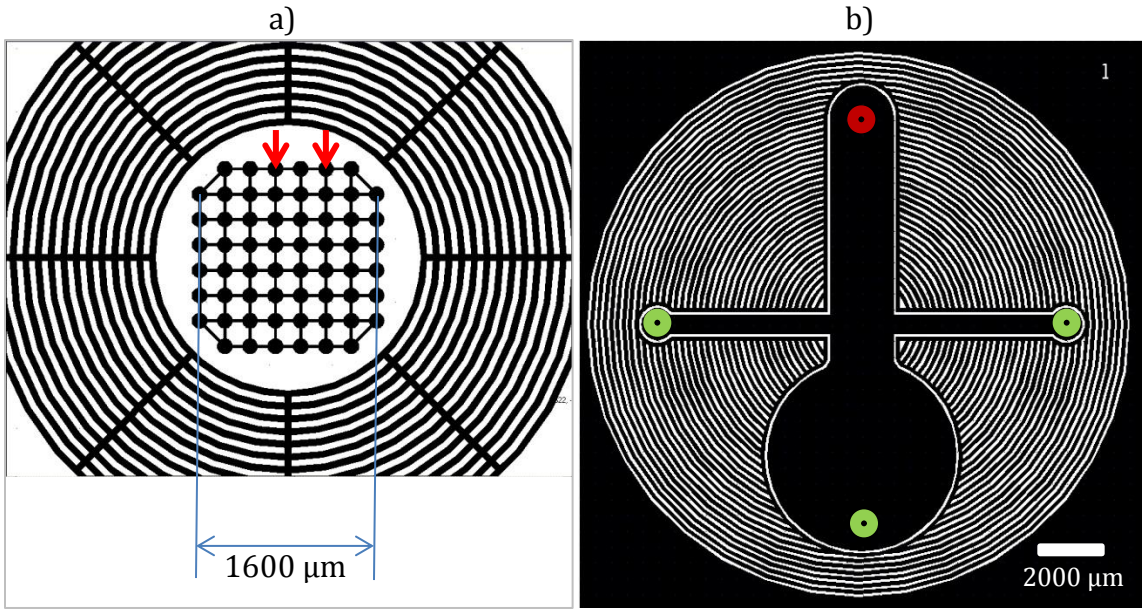

Fig. 1: The schematics of the µF device designs used for a) surface patterning and b) cell culture perfusion. In (a), the circular areas indicated with red arrows were r=30 µm and 200 µm apart. The channels between the circular areas were 20 µm wide. This layout aligns with commonly used 8x8 MEAs. In (b), the green and the red circles indicate the locations for the three fluid inlets and the waste outlet respectively. The large channel was 2000 µm wide, the narrower, side inlets were 600 µm wide.

2.4.2 Microelectrode array fabrication

Our initial integration tests were carried out on the commercial, silicon nitride (SiN) passivated MEAs (60MEA200/30iR-Ti and 60MEA200/30iR-ITO; Multi-Channel Systems GmbH, Reutlingen, Germany). However, due to the relative high cost, irreversible modification or fouling, the experimentation was switched to the in-house devices fabricated using the bi-layer lift off method [38]. The arrays consisted of 59 microelectrodes of 30 µm, arranged in an 8x8 grid. The conductive tracks of the MEA and the surface surrounding the microelectrodes were passivated with 500 nm layer of aluminium nitride (AlN) or SiN. The microelectrode layout and dimensions were similar to the commercial devices. Using these dimensions ensured that our MEAs could also be integrated with the Multi-Channel Systems MEA1060 amplifiers for recording electrophysiological data (for the MEA fabrication protocol, see supplementary section S.2).

2.4.3 Culture chamber modules

Culturing cells on the MEAs requires these devices to be integrated with culture chambers. These chambers were fabricated from poly(methyl methacrylate) (PMMA) or Nylon using a computer numerical control (CNC) machine. The chambers were 5 mm tall with inner diameter 1.7 cm and outer diameter of 2.6 cm. Each custom chamber featured four equally spaced, threaded openings. These openings allowed other parts to be securely attached to the culture rings via M5 threaded screws. Once fabricated, the chambers were washed with household detergent, aligned and attached to the MEA using the Orabond 1397PP double sided tape.

2.4.4 Reservoir plate module for µF device

Traditional multichannel (3 or more) perfusion of µF devices requires the use of two or more pumps with a fluid reservoir for each channel. This increases the physical experimental set-up, quickly becoming unpractical and unreliable. To try and keep the size of the system to a minimum, it was attempted to perfuse the µF device using passive methods such as gravity and surface tension driven perfusion (see the supplementary section S.3). Unfortunately, the passive methods, although advantageous due to their small size, proved too unreliable and prone to spontaneous flow termination. Thus, to keep the size of the experimental set-up to a minimum while connected to the external syringe pump, the media reservoirs were integrated into the MEA assembly. This was achieved through fabrication of the "reservoir plate". This component housed the three fluidic reservoirs and was used to physically press the µF device against the MEA surface., The reservoir module was designed to anchor to the culture chamber module using screws. The positioning of the reservoirs matched that of the µF device channel inlets. Importantly, as well as housing the media reservoirs, this module was also tasked with mechanically pressing the µF device against the MEA surface during the experiments (see section 2.4.5). The fabrication of the reservoir module is summarized in Fig. 2.

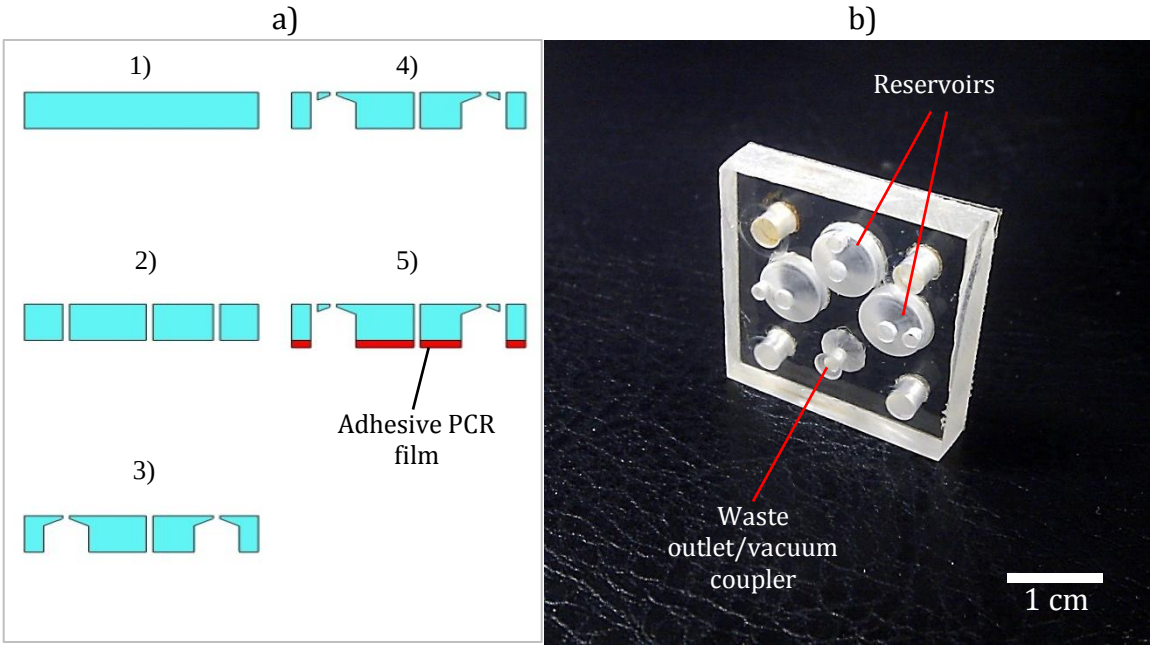

Fig. 2: a) The schematic of reservoir plate fabrication. 1) 5mm x 26 mm^2 PMMA block. 2) Drilling of the pilot openings. 3) Drilling of the reservoirs using the 7mm drill bit. 4) Drilling of the pressure release opening using 1.5 mm drill bit. 5) Attachment of the single sided adhesive PCR film (AB 0558) to the underside of the plate (red). This PCR film served as the gasket to ensure a watertight seal between the reservoir plate and the culture chamber. b) The image of fabricated reservoir plate complete with the opening for the M5 threaded bolts.

2.4.5 Fabrication of perfusion µF device modules

To achieve robust, reversible integration of the µF device with the MEA, this module was designed to fit tightly within the culture chambers (see section 2.4.3). These modules were fabricated using PDMS. The pre-polymer was mixed with the hardener at the ratio of 10:1, degassed and cured at 100 °C for 1 h. The fabrication of the µF modules for cell culture perfusion and its integration with an MEA is described in Fig. 3. To address specific practical issues, the µF device was fabricated in two molding steps. The first step ensured the good alignment of the microfluidic channels relative to the mold and the efficient degassing of PDMS in close proximity to the fluidic channels. The second molding step was used to fabricate a flat surface suitable for forming a functional watertight seal with the reservoir plate (see section 2.4.4).

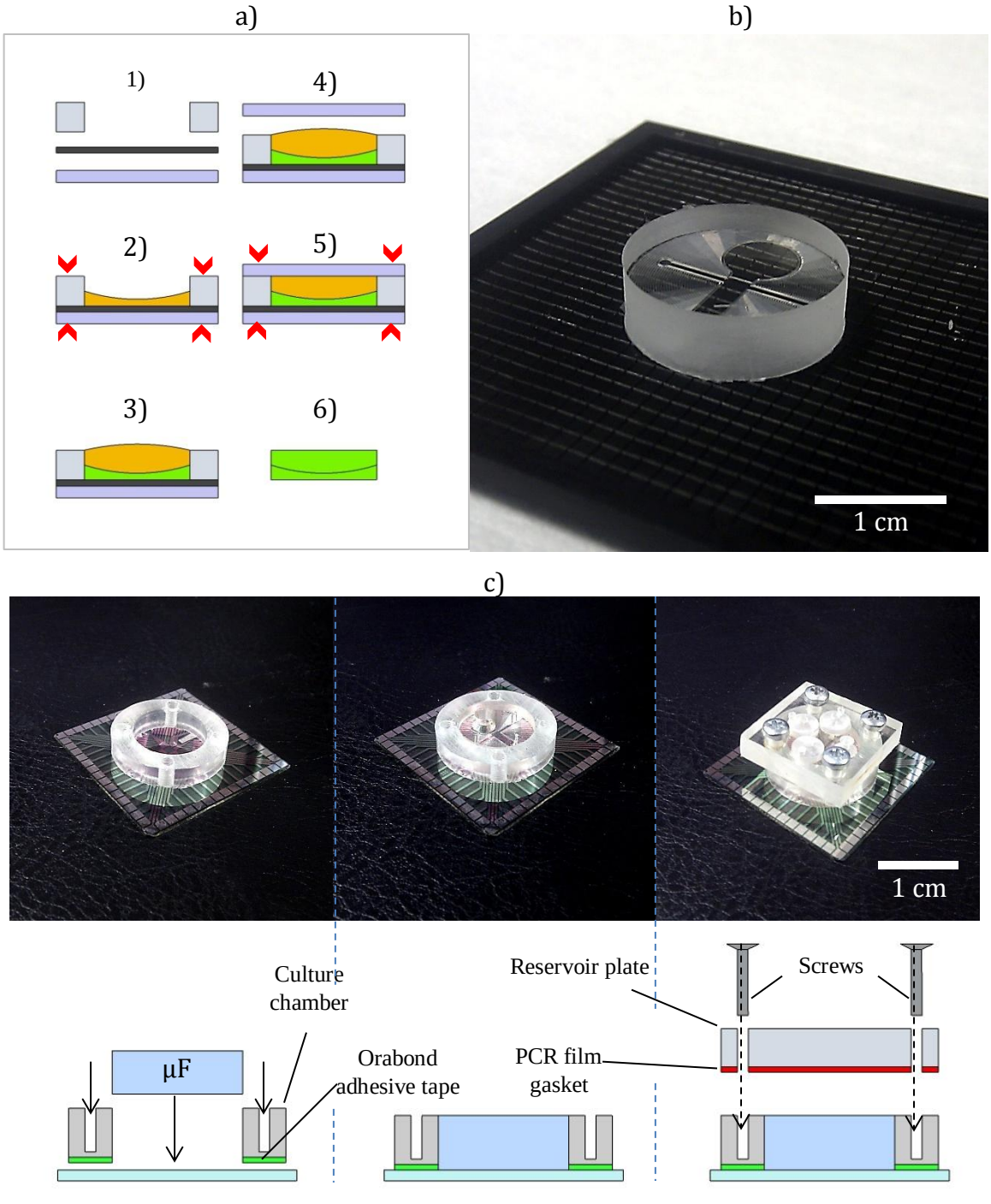

Fig. 3: a) The schematic of μF device fabrication: 1) the silicon master (black) is sandwiched between the Pyrex slide (blue) and a culture chamber (gray). 2) The assembly is clamped (red chevrons), the well is partially filled with pre-polymer PDMS (yellow), degassed and cured. 3) The clamps are removed and fresh pre-polymer PDMS (yellow) is poured onto the cured PDMS (green). 4) A second Pyrex slide is attached. 5) The slide is clamped and PDMS cured again. 6) After cure, the parts are disassembled to produce the μF device. b) The PDMS μF device fabricated using the steps in (a). c) The assembly sequence. The culture chamber is aligned and attached to the MEA. The μF device is inserted into the culture chamber. The reservoir plate is attached to the culture chamber with M5 screws.

2.5 Surface patterning

2.5.1 Alignment

To demonstrate that the modular µF system (Fig. 3) was compatible with patterning of surface chemistry, the MEAs were patterned with PDL and Fibronectin. The patterning was achieved by aligning a small µF device (**Fig. 1**(a)) with the microelectrodes and perfusing the channels with the polymer-protein solution. The alignment set up consisted of a rectangular base and lid with an opening in the centre. The alignment steps are shown in Fig. 4(a). The "vertical" and the "horizontal" 20 µm wide channels of the µF device (fixed to the platform on the aligner) were used as the alignment marks for the 30 µm electrodes on the MEA surface. The correct alignment placed the microelectrodes in the centres of the 60 µm circular chambers of the µF device (see supplementary section S.4).

2.5.2 Patterning

Once the patterned µF device was temporarily attached, it was filled with PDL-Fibronectin mix (1:1 mixture of 100 µg mL^{-1} PDL and 25 µg mL^{-1} Fibronectin in PBS) via PDMS vacuum treatment as previously described [39]. Briefly: the substrate with the attached µF device was placed into a vacuum (~ 100 mTorr) for 5 min. After vacuum exposure, two small drops of PDL-Fibronectin solution were placed onto the inlets of the µF device effectively blocking the access of air into the channels. As the pressure in the channels decreased, the drops of liquid were forced into the channels via ambient air pressure. The filled µF device was then incubated at 37 °C for 20 min. Following the incubation, the µF channels were rinsed by drawing a drop of DI water from one inlet into the channels using a lint free tissue. The µF device was then carefully removed leaving the patterned MEA (Fig. 4 (b))

a)

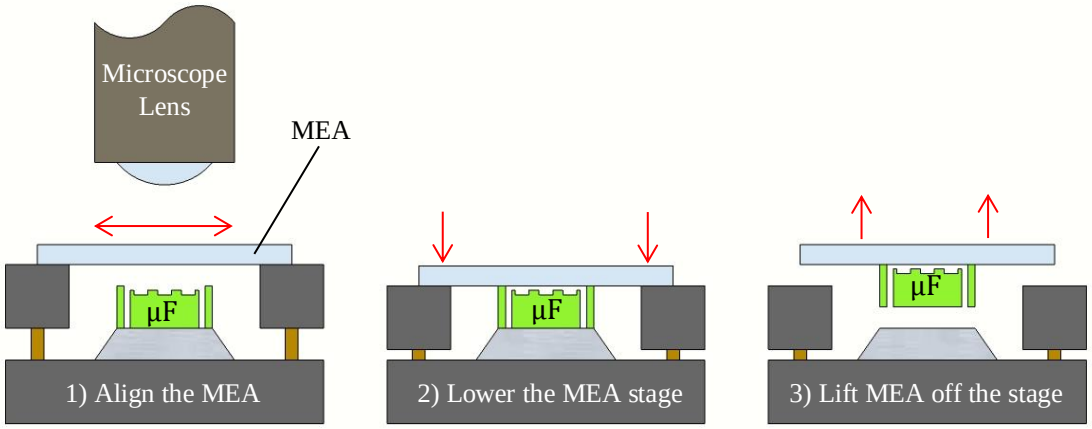

b)

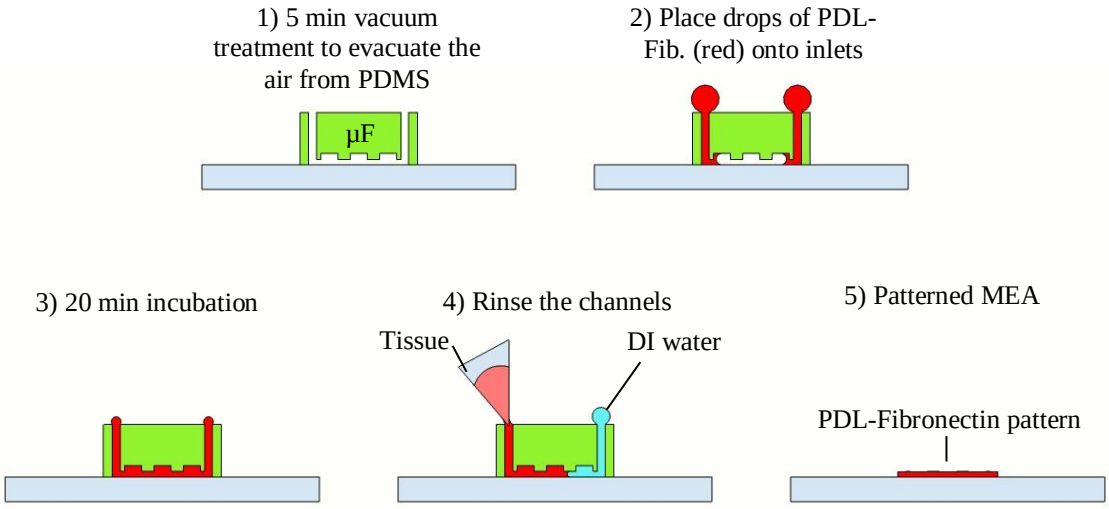

Fig. 4: a) The schematic of the basic steps involved in the alignment of the patterning microfluidic device (marked "µF") with the MEA. (1) With the aid of an upright microscope, the MEA is aligned with the µF device below it. (2) The nuts were tightened to bring the aligned MEA surface into contact with the µF device. Once the µF device is attached to the MEA, it can be lifted from the rig. b) The schematic representing the basic steps of MEA patterning via vacuum treatment of the µF device.

2.6 A549 cell culture

The A549 cells were used to demonstrate the concept of controlling the cell distribution within a microfluidic channel. These cells were selected due to their robustness and the high rate of division. The A549 cell line produces a confluent layer in 24 to 36 hours and is well suited for testing differential microfluidic environments.

The cells were cultured and split as per standard protocol. The A549 cells were seeded at a density of ~$3.5x10^5$ cells mL^{-1} in 700 µL of DMEM and were allowed to adhere to the substrate for 1h. Following the cell attachment, 500 µL of the cell culture media was removed and the µF device, which has been pre-soaked in HBSS for 48 h at 37 °C, was inserted into the well and secured via the reservoir plate. The pre-soaking in HBSS was used to saturate PDMS and reduce the chances of air bubble formation during perfusion. The µF device was perfused at rate of 10 µL h^{-1} with DMEM supplemented with 10% FBS from two separate reservoirs. The third reservoir was filled with DMEM without growth factor supplements. The A549 culture inside the T-75 flask was used as the control. The cell culture was imaged before and after µF perfusion using an inverted microscope

2.7 Primary neuronal culture

The neural cells were harvested from the spinal cords of Sprague Dawley rat embryos on the 14^{th} day of gestation (E14). The neuronal tissue was acquired as described elsewhere [40]. Briefly, a pregnant Sprague Dawley rat was anesthetized by inhalation of halogenated ether vapor in a bell jar. Tail pinch and eye rub tests were performed to ensure that the rat was unresponsive and did not feel pain. The rat was then killed by decapitation and the embryos were extracted via a cesarean section. The embryo neuronal tissue was dissected under a microscope and suspended in sterile HBSS prior to dissociation. In cases when the tissue had to remain un-dissociated for more than 30 min, it was suspended in cool Neurobasal media instead of HBSS. To dissociate the nervous tissue, it was incubated in 5 mL of trypsin at 37 °C for 5 min. To stop the action of trypsin, 500 µL of trypsin inhibitor or 500 µL of FBS was added to the tissue suspension. The tissue was dissociated by trituration using a P1000 Gilson pipette then the cell suspension was spun in a centrifuge for 5 min at 1100 rpm to separate the neuronal cells from the trypsin solution. After the spin, the supernatant was discarded and replaced with 1 mL of Neurobasal media. The pellet was gently triturated again for few minutes to re-suspend the cells in fresh media. The neurons were seeded onto the surface of the MEA at the density of $1x10^5$ cells cm^{-2} in 700 µL of Neurobasal media supplemented with 2% B27, 10% FBS and 10 µl ml^{-1} GlutaMAX. After 2 days in vitro (DIV) on the MEA surface, the HBSS saturated µF device was attached as described above and the neurons were perfused for 24 h at a volumetric rate of 5µL h^{-1}.

3 Results

3.1 Gradient controled cell distribution

Microfluidic gradients offer the potential to control cell population distribution based on their nutrient requirements.. Importantly, *in vivo*, the development of the structures of the central nervous system (CNS) is greatly influenced by the trophic factor gradients in the extracellular space, resulting in areas more suited to specific types of neuronal cells. This phenomenon is particularly important for electrophysiological experiments because the neuronal electrical activity is known to be influenced by the presence of other neuronal cell types [41, 42].

Prior to fabrication of the silicon masters and the µF devices, a COMSOL simulation of the channel perfusion was performed. The simulation was intended to provide a representation of the gradient formation during the perfusion of the µF device. The shape of the microfluidic gradient generated using the COMSOL simulations corresponded well with the gradient generated experimentally, inside the 2000 µm channel (Fig. 5 (a) and (b)).

Following the test of the gradient formation, the µF device module was used to control the distribution of A549 cells inside the channel. This test was intended to demonstrate that the reversibly attached µF device can be used effectively for generating a differential, cell culture environment. This capability of µF devices has been previously demonstrated using trypsin or SDS fluidic gradients [43-45]. However, rather than using potent detergents, it was demonstrated that the distribution of A549 cells can also be controlled via exclusion of growth factors (FBS and GlutaMAX) from a perfusing gradient. After 24 h, the population of A549 cells that were perfused with un-supplemented media was visibly reduced while the cells perfused with normally supplemented media did not show any obvious reduction in the population confluency (Fig. 5 (c-e)).

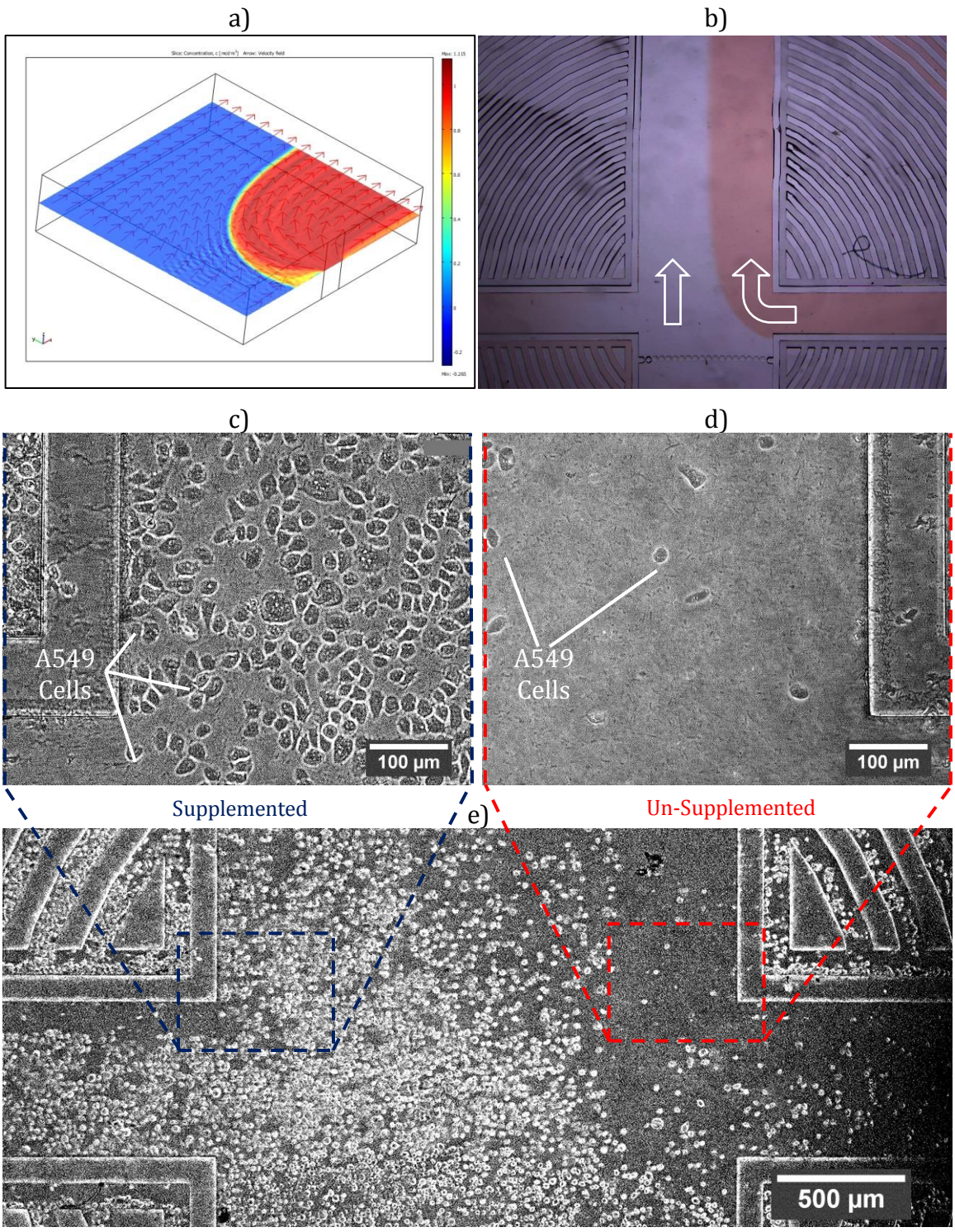

Fig. 5: a) COMSOL simulation of the µF device perfusion showing the formation of separate streams and laminar flow inside the fluidic channel and in close proximity to the side inlet (volumetric rate: 20 µL min^{-1}). b) The fluidic gradient generated using the µF device. The device dimensions were identical to those used in COMSOL simulation. The perfusion rate was set to 8 µL min^{-1}. c) A549s on the supplemented side after 24 h perfusion. d) A549 on the un-supplemented side after 24 h perfusion. e) Image showing the difference in A549 cell density relative to fluidic inlets.

3.2 Patterned neuronal growth

Patterning of neuronal cells *in vitro* using surface chemistry modifications is a well-established methodology [26, 27, 30, 46]. The guidance of neuronal growth using the surface chemistry and trophic factor gradients during the development of the CNS *in vivo*, is also well documented [47, 48]. In fact, the combination of the surface chemistry with the trophic factor gradients in the extracellular space plays one of the most important roles in the correct formation of the CNS architecture [49]. To demonstrate the neuronal patterning generated via surface patterning, the µF device (See Fig. 1(b)) was attached to the SiN coated Pyrex substrate by conformal contact. The microchannels were filled with the 100 µg mL^{-1} solution of PLL-FITC and incubated with the surface for a period of 20 min. After incubation, the µF device was removed and the substrate was imaged using a fluorescent microscope. Fig. 6 (a) shows the PLL-FITC pattern on SiN surface generated using µF patterning method. Seeding the primary neuronal cultures onto the PLL (a cell adhesion promoter) patterned substrate resulted in patterning of neuronal cells. The results are consistent with previous reports that used adsorbed polylysine on bare SiN surface [50, 51]. The neurons remained pattern compliant up to 13 DIV (Fig 6. (b) and (c)). The long term viability and compliance of neurons to the patterned surfaces is an important and promising result because after 12-14 DIV, the neurons form an extensive, electrically active network capable of spontaneous, synchronized electrical activity (See supplementary section S.5).

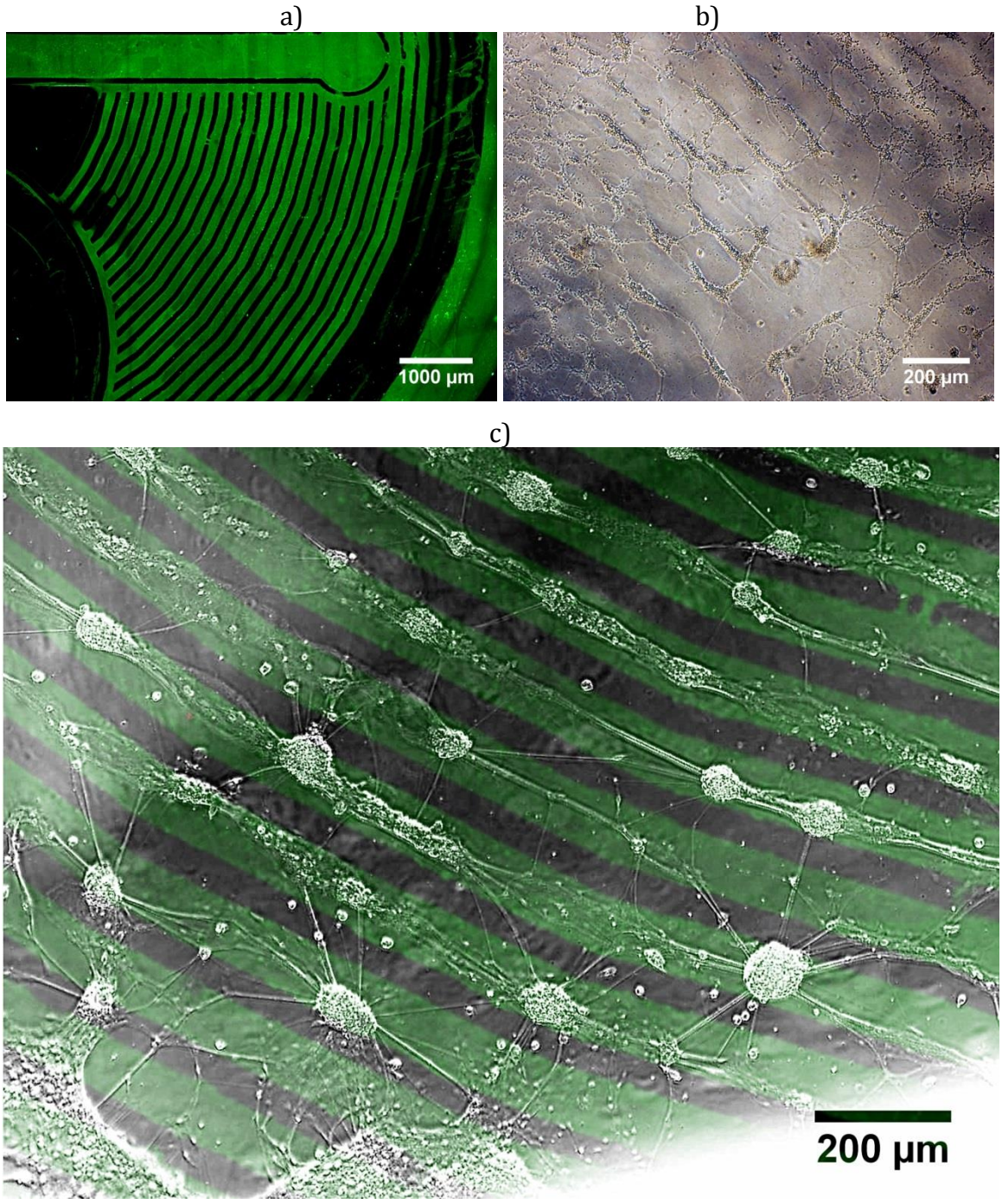

Fig. 6: The fluorescence images of surface patterns generated using the µF device perfused with a) fluorescein solution and b) patterned, E14 rat embryo spinal cord neurons on SiN coated Pyrex substrate at 2DIV (Substrate patterned with 100 µg mL^{-1} PLL). c) Patterned growth of E14 rat embryo spinal cord neurons at 13 DIV. The neuronal growth is compliant with the PLL-FITC patterned surface (green lines).

3.3 Reversible integration of µF device with patterned neurons on MEA surface

Following the separate experiments with the control of cell patterning and distribution on the Pyrex substrates, the surface of an MEA was patterned with PLL-fibronectin solution and used for culturing of patterned neurons inside the perfused, reversibly integrated microfluidic channel. The reversibility of the µF device attachment is of paramount importance because it allows the chemical patterning of the MEA surface.

Fig. 7(a) shows the neuronal culture prior to the attachment of the µF module. At this stage of the cell culture, the neuronal patterning is shown by the preferential attachment of cells to the PDL-Fibronectin pattern (green pattern). After 2DIV, the µF module was successfully integrated with the existing patterned culture and mechanically secured using the overlying PMMA culture chamber plate. The culture was then perfused for the 24 h period at a rate of 5 µL h^{-1} (Fig 7 (b)). The integration of the µF device did not have any obvious negative effects regarding the neuronal viability and pattern compliance. Interestingly, the µF device perfusion has resulted in a marked reduction in the number of dead, floating neurons (white arrows in Fig. 7(a)).

This result represents the first demonstration of an MEA simultaneously and reversibly integrated with a functional µF device and chemically patterned neuronal network. The reversible integration of the µF device, allows this assembly to sustain the culture in potentially more favorable static environment without sacrificing the ability to perform µF experiments. The aligned, reversible attachment of patterning and perfusing µF devices ensures that the microelectrodes are positioned inside the fluidic channels, avoiding the direct contact and contamination with PDMS. An additional benefit of the reversible attachment is the ability to remove the µF device, and carry out the remainder of the cell culture experiment under "normal", static conditions.

Importantly, this result also represents an in vitro system capable of controlling the formation of neuronal networks using the similar strategies to those found *in vivo* (surface chemistry and diffuse trophic factor gradients). The combination of these factors, allows a high degree of control over the *in vitro* neuronal cultures in terms of cell placement and types; thus, making it possible to build defined neuronal circuits consisting of required cell types. Further, the electrical activity of these neuronal circuits can be monitored or stimulated using the integrated MEA.

The combination of the above capabilities has produced a powerful, flexible, multifunctional research tool for experiments involving electrophysiology, neuronal guidance, neuromodulation, regenerative neuroscience or drug screening.

a)

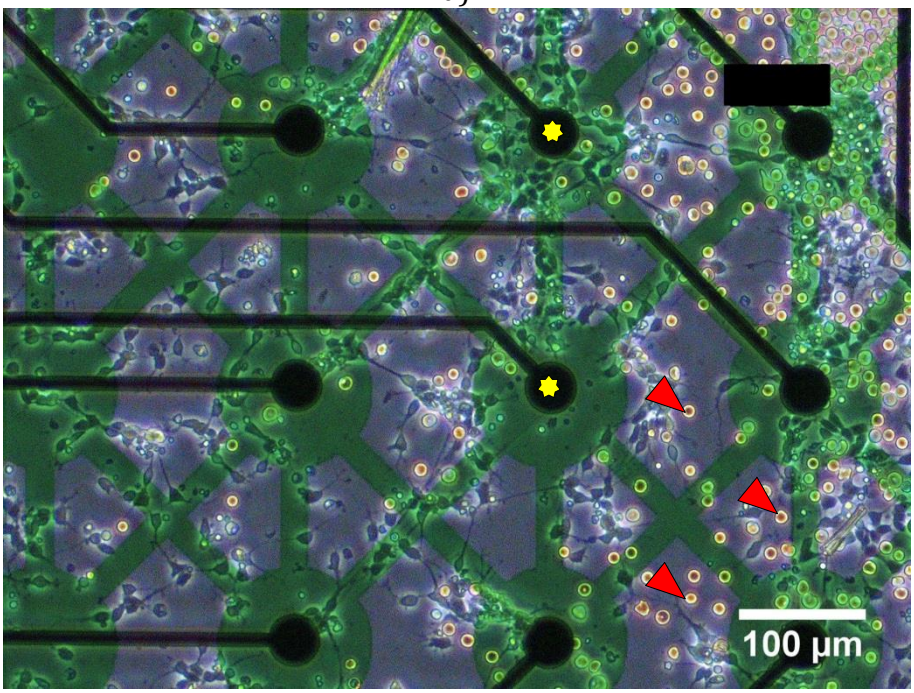

b)

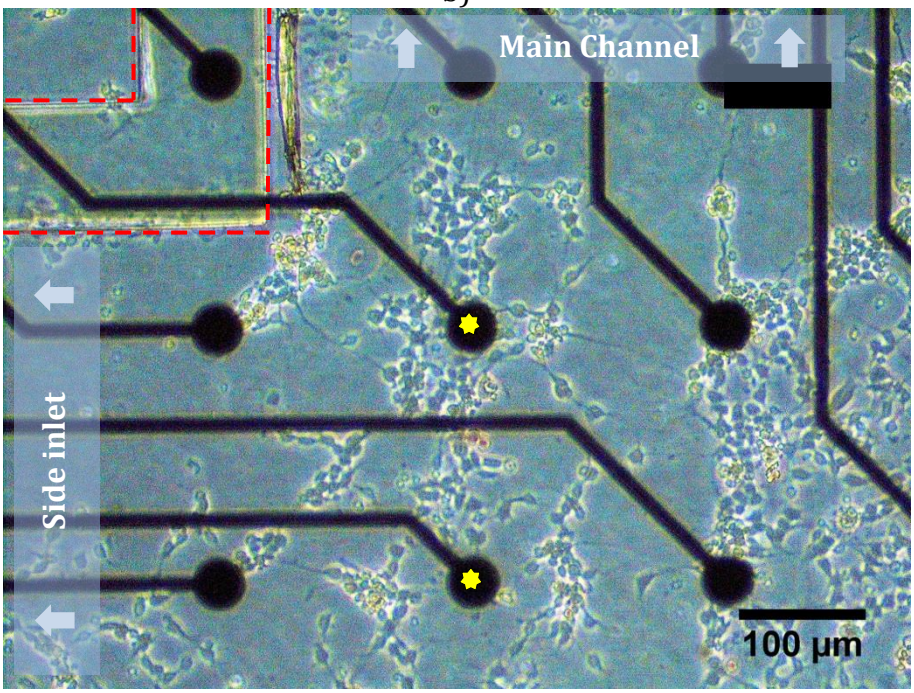

Fig. 7: a) Patterned neuronal network on the MEA surface. The green pattern indicates surface modifies with PDL-Fibronectin. The red arrows indicate the dead neurons, floating in the culture media. b) Neurons seen in (a) but with an integrated µF device. Note: images (a) and (b) show the same neuronal pattern. The yellow stars indicate the same electrodes. The red dashed lines indicate the µF channel wall where the side inlet (600 µm wide) meets the large (2000 µm wide), main channel.

4 Discussion

The aim of this study was to design and build a microfabricated system, capable of simultaneously controlling the distribution of neuronal cells using the combination of surface chemistry with the microfluidic gradients and monitor the neuronal electrophysiological activity. An additional aim was to address some of the practical issues associated with the integration of PDMS microfluidics with MEAs. Specifically, in our experience; the inconsistent bond of the µF devices with the substrate, the device re-usability and the resultant poor range of application, make it difficult to justify permanent µF integration with expensive, seemingly re-usable MEAs. Even though, it has been shown that PDMS can be strongly bonded to SiN [52], this step narrows the range of application to experiments that do not require chemical surface patterning or multiple cell culture experiments. To date, only a small number of studies have attempted to address the issues associated with permanent PDMS bonding [31, 53]. Hence, this study described an alternative method of secure, reversible integration of the µF device with the MEA. This was achieved by fabricating a number of modules designed to physically press the PDMS µF device against the selected substrate. The permanently attached culture chamber module served to confine the µF device in the XY plane. However, if an alternative or new experimental design does not require the integrated microfluidics, this module can also be used as the conventional culture well, reverting the MEA to the original specification; and thus, maintaining a wider scope of application.

The reservoir plate module served to press the µF device down against the surface. In addition, this module housed the media reservoirs which also resulted in reduced size of the setup. To avoid subjecting the chamber-MEA bond to excessive hydraulic pressure during perfusion, the system utilized suction to draw the media from the reservoirs through the µF channels making this system less prone to leaks.

To demonstrate the functionality of this set up, we used the reversibly attached µF device to control the distribution of A549 cells on a Pyrex substrate. Following this, by culturing patterned neuronal population on the MEA integrated with the µF device, we demonstrated that this methodology allows for a more flexible experimental setup that is not subject to substrate µF device bond.

This type of reversible integration has resulted in a multifunctional, integrated system, geared toward multiple neurobiological experiments. Specifically, our method allows the simultaneous integration of the MEA with chemical surface patterning, patterned neuronal cultures and multichannel microfluidic perfusion. Importantly, because the PDMS µF device does not have to mechanically support the perfusion lines, the assembled system proved to be user friendly and able to withstand extensive manual handling. The reversible µF integration with the MEA enables this system to 1) record or stimulate neuronal electrical activity as well as focally electroporate the cells on the surface [54]; 2) modify and pattern the surface chemistry to suit the experimental demands; 3) use the modified surface chemistry to control the neuronal network development 4) control the cell culture environment via microfluidic gradients; 5) test multiple µF device layouts during any stage of the cell culture and 6) monitor the microfluidic network in real time using conventional inverted microscopy techniques.

The above capabilities enable this system to be used for different experiments involving any combination of the following: cell culture, cell types, electrophysiology, transfection, cell staining, surface chemistry,

microfluidics and microscopy. The integrated system of this type has the potential to be applied to research in the fields of regenerative neuroscience or spinal cord injury for example. The ability to control the surface and fluidic environment of the neuronal culture is very useful because it is closely related to the *in vivo* models of neuronal growth and development [55]. The additional capability of this platform to record the neuronal electrical activity can be utilised to determine if the anatomical regeneration was accompanied by functional connectivity between the severed neurons. Alternatively, this platform can be applied to experiments involving neuromodulation. The added benefit is that the modulatory effects of various compounds can be focused on the selected parts of the neuronal culture using the microfluidic gradients. The effects of focal neuromodulation can then be measured by comparing the electrophysiological data.

5 Conclusion

This study has focused on designing and testing an alternative method of integrating the µF devices with MEAs to create a system with a broad scope of application. It was successfully demonstrated that the distribution of the A549 cells inside the channels of reversibly attached µF device can be controlled via fluidicgrowth factor supplement gradients. Furthermore, the compatibility of the reversible µF integration with MEAs and patterned neuronal networks *in vitro* wasdemonstrated. These results show that this methodology can potentially be used to construct a multifunctional, modular research tool geared towards experiments with electrophysiology, neuronal guidance and microfluidics.

6 Acknowledgements

This research was funded by the Program for Research in Third-Level Institutions (PRTLI) and the National Biophotonics and Imaging Platform Ireland (NBIPI).

Paul Galvin acknowledges the financial support of Science Foundation Ireland (SFI) under grant numbers SFI/12/RC/2289, SFI 12/RC/2272, SFI 10/CE/B1821 and SFI 07/CE/I1147.

References

1. Vulto, P., P. Kuhn, and G.A. Urban, *Bubble-free electrode actuation for micro-preparative scale electrophoresis of RNA.* Lab on a Chip, 2013. **13**: p. 2931-2936.
2. Lin, S.-C., et al., *A low sample volume particle separation device with electrokinetic pumping based on circular travelling-wave electroosmosis.* Lab on a Chip, 2013. **13**: p. 3082-3089.
3. Schimek, K., et al., *Integrating biological vasculature into a multi-organ-chip microsystem.* Lab on a Chip, 2013. **13**: p. 3588-3598.

4. Beebe, D.J., G.A. Mensing, and G.M. Walker, *Physics and applications of microfluidics in biology.* Annual review of biomedical engineering, 2002. **4**(1): p. 261-286.
5. Stone, H.A., A.D. Stroock, and A. Ajdari, *Engineering flows in small devices.* Annual Review of Fluid Mechanics, 2004. **36**(1): p. 381-411.
6. Whitesides, G.M., *The origins and the future of microfluidics.* Nature, 2006. **442**(7101): p. 368-373.
7. Mellors, J.S., et al., *Fully Integrated Glass Microfluidic Device for Performing High-Efficiency Capillary Electrophoresis and Electrospray Ionization Mass Spectrometry.* Analytical Chemistry, 2008. **80**(18): p. 6881-6887.
8. Chandrasekaran, A., et al., *Hybrid integrated silicon microfluidic platform for fluorescence based biodetection.* Sensors, 2007. **7**(9): p. 1901-1915.
9. Illa, X., et al., *A cyclo olefin polymer microfluidic chip with integrated gold microelectrodes for aqueous and non-aqueous electrochemistry.* Lab on a Chip, 2010. **10**(10): p. 1254-1261.
10. Narasimhan, J. and I. Papautsky, *Polymer embossing tools for rapid prototyping of plastic microfluidic devices.* Journal of Micromechanics and Microengineering, 2004. **14**(1): p. 96.
11. Rolland, J., et al., *Functional perfluoropolyethers as novel materials for microfluidics and soft lithography.* POLYMER PREPRINTS-AMERICA-, 2004. **45**(2): p. 106-107.
12. Rolland, J.P., et al., *Solvent-Resistant Photocurable "Liquid Teflon" for Microfluidic Device Fabrication.* Journal of the American Chemical Society, 2004. **126**(8): p. 2322-2323.
13. Nge, P.N., C.I. Rogers, and A.T. Woolley, *Advances in Microfluidic Materials, Functions, Integration, and Applications.* Chemical Reviews, 2013. **113**(4): p. 2550-2583.
14. Makamba, H., et al., *Surface modification of poly(dimethylsiloxane) microchannels.* Electrophoresis, 2003. **24**(21): p. 3607-3619.
15. Zhou, J., A.V. Ellis, and N.H. Voelcker, *Recent developments in PDMS surface modification for microfluidic devices.* Electrophoresis, 2010. **31**(1): p. 2-16.
16. Anderson, J.R., et al., *Fabrication of Topologically Complex Three-Dimensional Microfluidic Systems in PDMS by Rapid Prototyping.* Analytical Chemistry, 2000. **72**(14): p. 3158-3164.
17. Flachsbart, B.R., et al., *Design and fabrication of a multilayered polymer microfluidic chip with nanofluidic interconnects via adhesive contact printing.* Lab on a Chip, 2006. **6**(5): p. 667-674.
18. Bhattacharya, S., et al., *Studies on surface wettability of poly (dimethyl) siloxane (PDMS) and glass under oxygen-plasma treatment and correlation with bond strength.* Microelectromechanical Systems, Journal of, 2005. **14**(3): p. 590-597.
19. Chang, J. and B. Wheeler, *Pattern Technologies for Structuring Neuronal Networks on MEAs*, in *Advances in Network Electrophysiology*, M. Taketani and M. Baudry, Editors. 2006, Springer US. p. 153-189.
20. Multi-Channel-Systems. *MEA Manual*. [PDF] 2011 [cited 2012 29/06]; Available from:

http://www.multichannelsystems.com/sites/multichannelsystems.com/files/documents/manuals/MEA_Manual.pdf.
21. Xu, B., F. Arias, and G.M. Whitesides, *Making Honeycomb Microcomposites by Soft Lithography.* Advanced Materials, 1999. **11**(6): p. 492-495.
22. De Gennes, P.G., *Polymer solutions near an interface. Adsorption and depletion layers.* Macromolecules, 1981. **14**(6): p. 1637-1644.
23. Auvray, L., M. Cruz, and P. Auroy, *Irreversible adsorption from concentrated polymer solutions.* J. Phys. II France, 1992. **2**(5): p. 1133-1140.
24. Park, J., H.S. Kim, and A. Han, *Micropatterning of poly (dimethylsiloxane) using a photoresist lift-off technique for selective electrical insulation of microelectrode arrays.* Journal of Micromechanics and Microengineering, 2009. **19**: p. 065016.
25. Maghribi, M., et al. *Stretchable micro-electrode array [for retinal prosthesis]*. in *Microtechnologies in Medicine; Biology 2nd Annual International IEEE-EMB Special Topic Conference on*. 2002.
26. Chang, J.C., G.J. Brewer, and B.C. Wheeler, *A modified microstamping technique enhances polylysine transfer and neuronal cell patterning.* Biomaterials, 2003. **24**(17): p. 2863-2870.
27. Corey, J.M. and E.L. Feldman, *Substrate patterning: an emerging technology for the study of neuronal behavior.* Experimental Neurology, 2003. **184**: p. 89-96.
28. Sorribas, H., C. Padeste, and L. Tiefenauer, *Photolithographic generation of protein micropatterns for neuron culture applications.* Biomaterials, 2002. **23**(3): p. 893-900.
29. Beaulieu, I., M. Geissler, and J. Mauzeroll, *Oxygen Plasma Treatment of Polystyrene and Zeonor: Substrates for Adhesion of Patterned Cells.* Langmuir, 2009. **25**(12): p. 7169-7176.
30. Suzuki, M., et al., *Neuronal cell patterning on a multi-electrode array for a network analysis platform.* Biomaterials, 2013. **34**(21): p. 5210-5217.
31. Biffi, E., et al., *Validation of long-term primary neuronal cultures and network activity through the integration of reversibly bonded microbioreactors and MEA substrates.* Biotechnology and Bioengineering, 2012. **109**(1): p. 166-175.
32. Natarajan, A., et al., *Patterned cardiomyocytes on microelectrode arrays as a functional, high information content drug screening platform.* Biomaterials, 2011. **32**(18): p. 4267-4274.
33. Morin, F.O., Y. Takamura, and E. Tamiya, *Investigating neuronal activity with planar microelectrode arrays: achievements and new perspectives.* Journal of bioscience and bioengineering, 2005. **100**(2): p. 131-143.
34. Laermer, F. and A. Schilp, *Method of anisotropic etching of silicon*, U.S.P. Office, Editor. 2003, Robert Bosch GmbH (Stuttgart, DE) USA.
35. Li, N., C. Sip, and A. Folch, *Microfluidic chips controlled with elastomeric microvalve arrays.* Journal of visualized experiments: JoVE, 2007(8).
36. Qin, D., Y. Xia, and G.M. Whitesides, *Soft lithography for micro- and nanoscale patterning.* Nat. Protocols, 2010. **5**(3): p. 491-502.

37. Sidorova, J.M., et al., *Microfluidic-assisted analysis of replicating DNA molecules.* Nature protocols, 2009. **4**(6): p. 849-861.
38. Golden, J., et al., *Optimization of Bi-layer Lift-Off Resist Process.* CS Mantech Technical Digest, 2009.
39. Cira, N.J., et al., *A self-loading microfluidic device for determining the minimum inhibitory concentration of antibiotics.* Lab on a Chip, 2012.
40. Streit, J., et al., *The generation of rhythmic activity in dissociated cultures of rat spinal cord.* European Journal of Neuroscience, 2001. **14**(2): p. 191-202.
41. Shi, M., et al., *Glia Co-Culture with Neurons in Microfluidic Platforms Promotes the Formation and Stabilization of Synaptic Contacts.* Lab on a Chip, 2013.
42. Park, J., et al., *Multi-compartment neuron-glia co-culture platform for localized CNS axon-glia interaction study.* Lab on a Chip, 2012.
43. Nie, F.-Q., et al., *On-chip cell migration assay using microfluidic channels.* Biomaterials, 2007. **28**(27): p. 4017-4022.
44. Villa-Diaz, L.G., et al., *Microfluidic culture of single human embryonic stem cell colonies.* Lab on a Chip, 2009. **9**(12): p. 1749-1755.
45. Lee, C.Y., E.V. Romanova, and J.V. Sweedler, *Laminar stream of detergents for subcellular neurite damage in a microfluidic device: a simple tool for the study of neuroregeneration.* JOURNAL OF NEURAL ENGINEERING, 2013. **10**(3): p. 036020.
46. Ricoult, S.G., et al., *Generation of microisland cultures using microcontact printing to pattern protein substrates.* Journal of Neuroscience Methods, 2012. **208**(1): p. 10-17.
47. Endo, Y. and J.S. Rubin, *Wnt signaling and neurite outgrowth: Insights and questions.* Cancer Science, 2007. **98**(9): p. 1311-1317.
48. Lee, W.-H., S. Javedan, and C.A. Bondy, *Coordinate expression of insulin-like growth factor system components by neurons and neuroglia during retinal and cerebellar development.* The Journal of neuroscience, 1992. **12**(12): p. 4737-4744.
49. Walsh, F.S. and P. Doherty, *NEURAL CELL ADHESION MOLECULES OF THE IMMUNOGLOBULIN SUPERFAMILY: Role in Axon Growth and Guidance.* Annual Review of Cell and Developmental Biology, 1997. **13**(1): p. 425-456.
50. Chang, J.C., G.J. Brewer, and B.C. Wheeler, *Modulation of neural network activity by patterning.* Biosensors and Bioelectronics, 2001. **16**(7-8): p. 527-533.
51. Nam, Y., et al. *Electrical stimulation of patterned neuronal networks in vitro*. in *Engineering in Medicine and Biology Society, 2003. Proceedings of the 25th Annual International Conference of the IEEE*. 2003.
52. Tang, K., et al. *Evaluation of bonding between oxygen plasma treated polydimethyl siloxane and passivated silicon*. in *Journal of Physics: Conference Series*. 2006. IOP Publishing.
53. Tkachenko, E., et al., *An easy to assemble microfluidic perfusion device with a magnetic clamp.* Lab on a Chip, 2009. **9**(8): p. 1085-1095.
54. Jain, T. and J. Muthuswamy, *Microsystem for transfection of exogenous molecules with spatio-temporal control into adherent cells.* Biosensors and Bioelectronics, 2007. **22**(6): p. 863-870.

55. Dodd, J. and T.M. Jessell, *Axon guidance and the patterning of neuronal projections in vertebrates.* Science, 1988. **242**(4879): p. 692-699.
56. Kim, S.-J., et al., *Passive Microfluidic Control of Two Merging Streams by Capillarity and Relative Flow Resistance.* Analytical Chemistry, 2005. **77**(19): p. 6494-6499.
57. Berthier, E. and D.J. Beebe, *Flow rate analysis of a surface tension driven passive micropump.* Lab on a Chip, 2007. **7**(11): p. 1475-1478.
58. Xing, S., R.S. Harake, and T. Pan, *Droplet-driven transports on superhydrophobic-patterned surface microfluidics.* Lab Chip, 2011.

7 Supplementary Section

S.1 Fabrication of silicon masters

The silicon masters for μCP stamps and the microfluidic devices were fabricated in-house fabrication facility. The very first step in this process was the drawing of the concept sketch using Google Sketch Up software. This stage outlined basic dimensions and features of masters to be manufactured. The sketch was then redrawn into a precise set of mask blueprints in AutoCAD by a qualified computer aided design (CAD) technician. The fabrication of masks was outsourced to Compugraphics, UK. Once the masks were fabricated, the silicon masters were fabricated by a qualified engineer via the following steps. A blank, new wafer was cleaned using the standard Radio Corporation of America (RCA) cleaning method. The RCA clean was designed to remove organic, inorganic and metal contaminants from the wafer surface without attacking the silicon itself (Kern, 1970). To define the master features, AZ 9260 resist was applied to the wafer and exposed through a photo-mask. The exposed photoresist was developed using HPRD 402 developer. Using the Bosch process, the wafers were etched to the depth of 10 and 15 μm for the μCP stamps and 100μm for the μF devices. The Bosch process involves a sequence of etch and passivation steps (Laermer and Schilp, 2003). The etch steps were 5 sec long utilizing sulfur hexafluoride (SF_6) plasma followed immediately by 2 sec. passivation with Octafluorocyclobutane (C_4F_8). The depth is controlled by the number of etch-passivation cycles performed. This method allows for creation of high aspect features in silicon crystal. After etch, the remaining photoresist was stripped by a combination of plasma and Piranha solution. All the steps above were performed by a trained silicon fabrication engineers.

S.2 Fabrication of MEAs using the bi-layer method

The MEA fabrication was carried out as follows: first, 4" Pyrex wafers (1 mm thick) were spin-coated with Hexamethyldisilazane (HMDS) primer at 4000 RPM for 50 sec to improve photoresist adhesion followed by spin-coating of Polymethylglutarimide (PMGI) resist. The wafer was then baked on a hotplate at 170 °C for 3 min. Following the resist bake, HDMS was spin-coated onto PMGI at 4000 RPM for 50 sec followed by spin-coating of Microposit S1813 imaging resist at 4000 RPM for 50 sec. The wafer was then baked on a hotplate at 115 °C for 2 min.

The wafers were then exposed to metal level photo-mask (this mask defined the layout of the microelectrodes, conductive tracks and contact pads) in Karl Suss MA1006 mask aligner at 70mW cm^{-2}, developed in Microposit 319 developer, rinsed in running DI water and oven baked at 90 °C for 30 min.

Following the resist patterning, the wafers were treated with Ar plasma for 30 sec and $2x10^{-7}$ Torr in an evaporator to improve metal adhesion. Ti:Pt (10nm:100nm) was then evaporated onto the wafer at 80 °C.

The metal lift off was performed at 80 °C in Microposit R1165 resist stripper. The metal patterned wafers were then rinsed in DI water before deposition of passivation coatings.

Following the metal lift of, each device was coated with either: SiN, AlN or polyimide passivation. 500nm SiN passivation was deposited onto the devices by chemical vapour deposition (CVD) in STS310 PECVD system. AlN was deposited at the thickness of 650 nm by sputtering in Oxford Instruments Plasmalab 400 Magnetron Sputtering system. Polyimide was spin-coated onto the devices at thickness of 6 µm and cured in a vacuum oven at 250 °C.

The patterning of passivation coating was carried out as follows: The SiN and AlN passivation layers were patterned using the same procedure as described for metal deposition and patterning. However, the assisting layer of PMGI resist was omitted. An appropriate passivation level photo-mask was aligned with the metal features of the MEA. This photo-mask defined the areas that are free from passivation, i.e. the microelectrodes and contact pads. Polyimide was patterned using 7 µm thick layer of AZ9260 photoresist instead of Microposit S1813 photoresist.

After resist patterning, SiN passivation was etched in STS Inductively Coupled Plasma (ICP) using CF_4/CHF_3 chemistry. AlN passivation was etched via reactive ion etching (RIE) in Oxford Instruments RIE Plasmalab System100 using BCl_3 chemistry. And finally, Polyimide was etched in ICP system using O_2/SF_6 chemistry. Following the passivation etch, the remaining resist was stripped using R1165 resist stripper and devices thoroughly rinsed in DI water.

S.3 Microfluidic perfusion-method testing

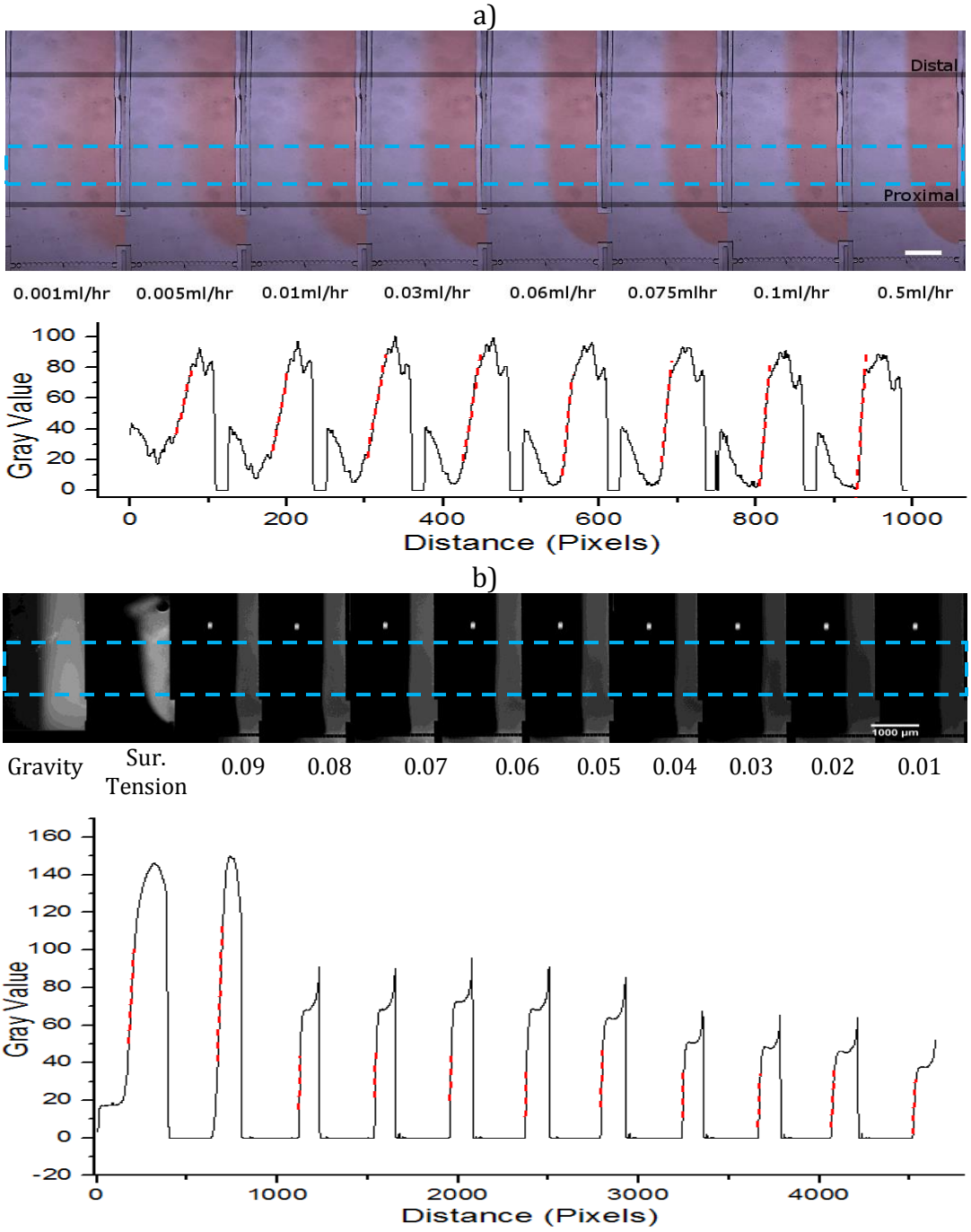

Fig. S1: The experimental comparison between the µF perfusion methods (hydrostatic pressure, liquid drop surface tension, syringe pump and peristaltic pump). a) Sequential images of gradients generated using the syringe pump. The volumetric rate was sequentially increased and the corresponding luminescence profiles (n=3) were measured. b) Sequence of images of fluidic gradients generated using gravity [e.g 56], surface tension [57, 58] and a peristaltic pump. The numbers 0.01-0.09 indicate the RPM setting of the peristaltic pump. The blue, dashed areas represent the pixels used for gathering the horizontal luminescence/fluorescence profiles. The red lines in the graphs indicate the gradient slopes. Scale bars: a) 650 µm, b) 1000 µm.

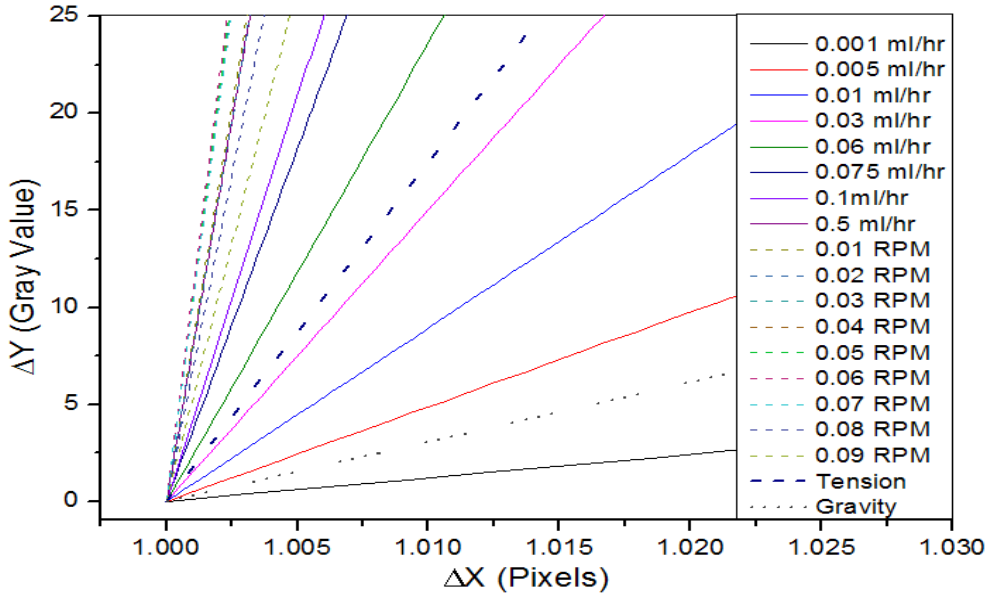

740

741 **Fig. S2**: Graph of gradient slopes measured from the fluorescence and luminescence intensity profiles
742 of fluidic gradients. Solid slopes represent gradients generated with a syringe pump; thin dashed
743 lines represent the gradients generated with a peristaltic pump. This data was used to determine the
744 volumetric rates generated by the passive perfusions methods (Gravity and surface tension driven).

745 Table T1: Perfusion method observations

Perfusion Method	Positive aspects	Negative aspects
Gravity Driven Perfusion	Small, simple and cheap No external power supply Potential 24 h perfusion Potential for perfusion with multiple channels (more than 2) Low volumetric rate Large reservoir volumes	Prone to spontaneous perfusion termination and bubble formation. Requires precise machining to control vol. rates. Difficult to load with perfusing solution
Surface Tension Driven Perfusion	Requires no extra equipment Reasonably low volumetric rate Gradients easily imaged using upright and inverted microscopes	Prone to spontaneous perfusion termination and bubble formation V. poor control over initiation of perfusion Incapable of long term perfusion due to low reservoir volumes Difficult to load the device with perfusing solution, requires steady hands and good dexterity
Syringe pump	Very good control of volumetric rate Consistent Two channel perfusion Large reservoir volume Long term perfusion (2-3 Days) “Withdraw” function (model specific)	The setup is bulky and time consuming Requires an external power supply Limited to number of channels (depending on the unit). Hard to integrate with tissue culture
Peristaltic pump	Good control of volumetric rate Bi-directional perfusion Less bulky than the syringe pump Two channel perfusion Large reservoir volumes	The minimum volumetric rate is high as compared to syringe pump. Requires an external power supply

	Long term perfusion (2-3 Days)	

S.4 Surface patterning comparison between µF and µCP

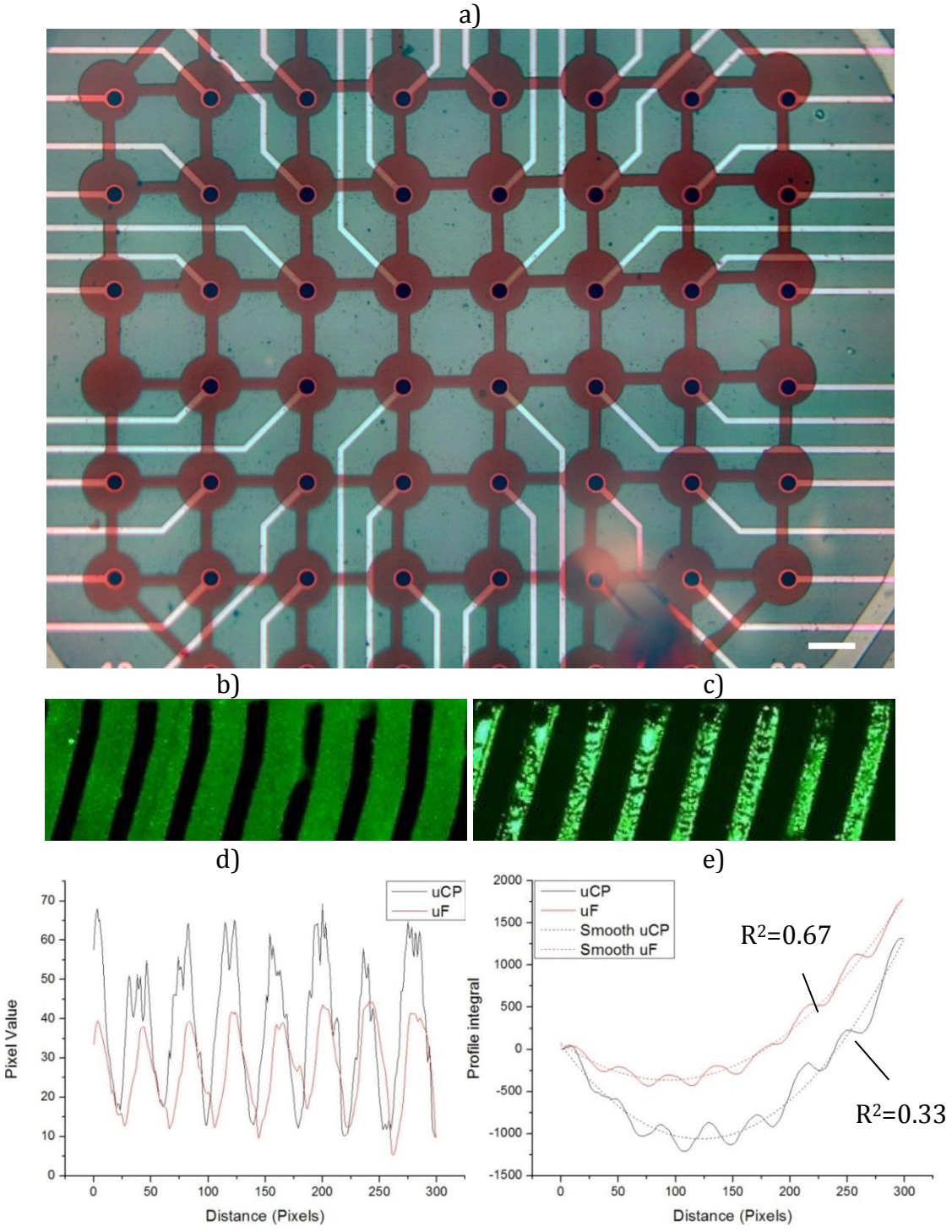

Fig. S3: Aligned µF patterning on MEA showing that the features of the µF device (e.g. the 60 µm circular chambers (red)) can be reliably aligned with the 30 µm microelectrodes (black) using the alignment setup and the upright microscope. Direct comparison of b) µF pattern with identical c) µCP pattern. d) Fluorescence profile comparison plot of (b) and (c). e) Integrated fluorescence data comparing the degree of feature recurrence (perfect recurrence: $R^2=1$).

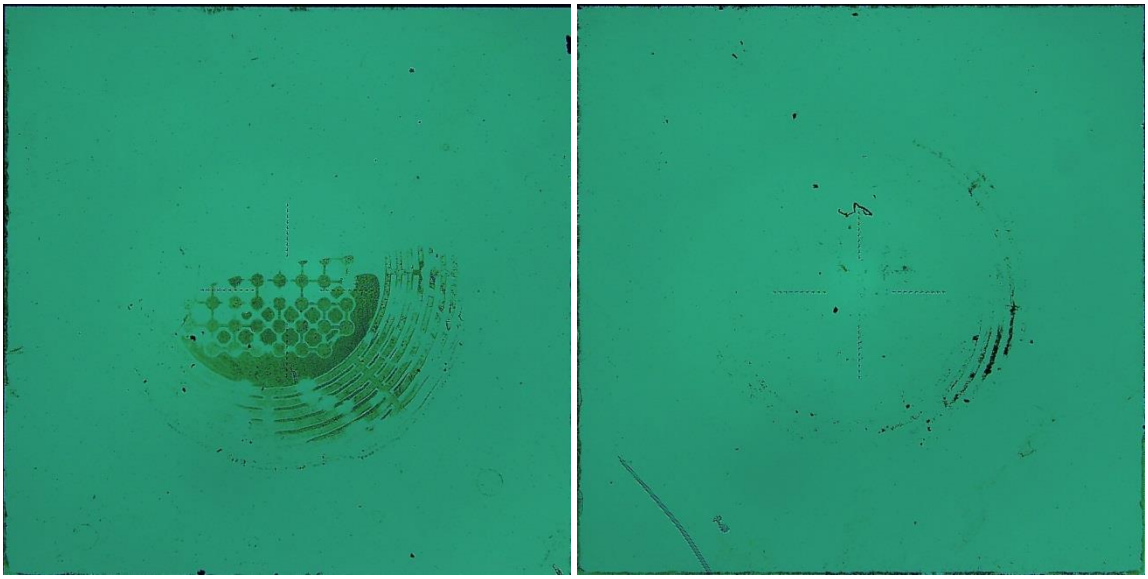

Fig. S4: Surface contamination with PDMS following the conformal contact during μCP. The deposition of the PDMS on microelectrodes has a negative effect on the electrode impedance and noise levels.

S. 5 Electrophysiological recordings-testing the commercial MEA

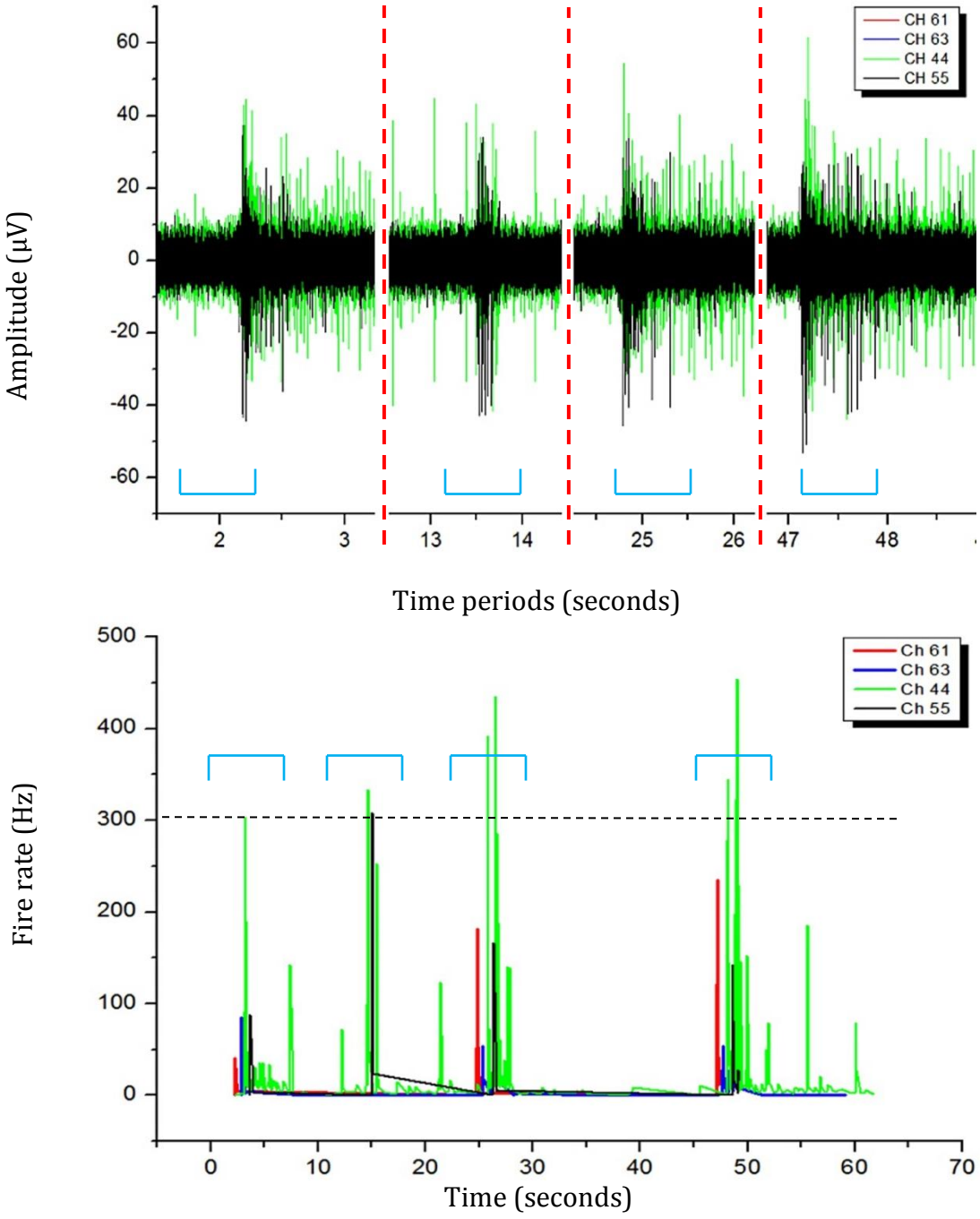

Fig. S5: a) Recorded signals from E14 rat embryo spinal cord at 14 DIV using the commercial, un-patterned MEA (60MEA200/30iR-Ti). The initial seeding density was $5x10^5$ cells cm^{-2}. The recorded signals show good synchronization between channels 44, 55 and 61. The red vertical lines separate the timeframes that show electrical synchronization (blue indicator). b) Graph showing action potential fire-rate comparison. The simultaneous increase of fire rates in channel 44 (green) and 55 (black) and to a lesser extent in 61 (red) indicates the synchronization electrical activity. Each recording was kept to a maximum of two minutes to avoid excessive file sizes. The sampling rate was

776 set to 40 kHz. Filtering (200 Hz high pass) and signal processing were performed off line using MC
777 rack software.

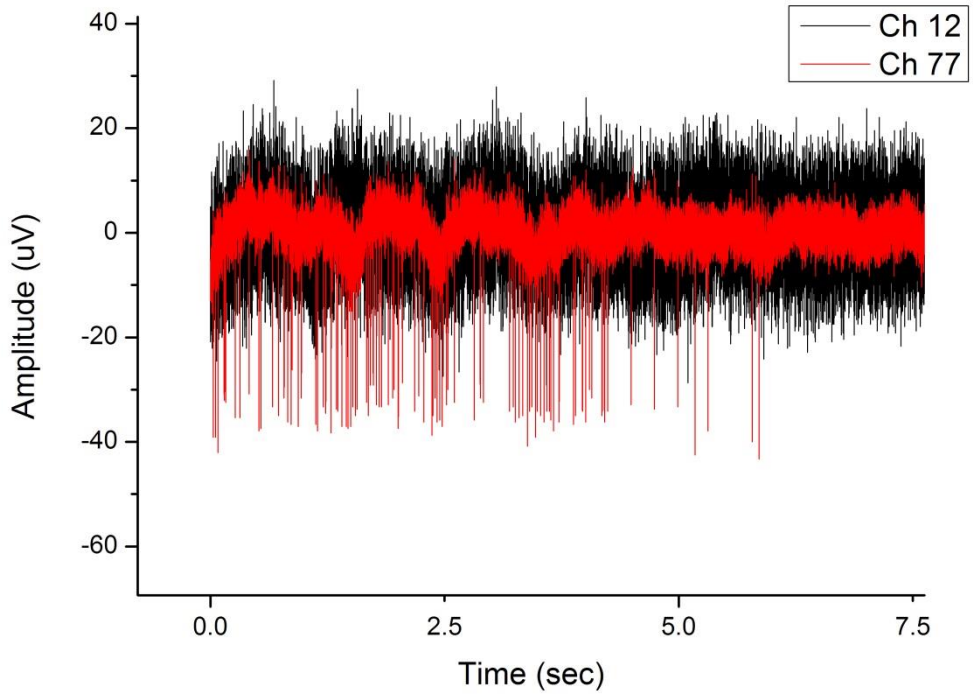

778

779 **Fig. S6**: The comparison of signal noise levels. The normal noise level (red trace) of +/- 10 µV is
780 superimposed over the recording from a "noisy" electrode on the same array. The Ch. 12 baseline
781 noise level was +/- 20 µV.

782